Electrochemistry Communications 135 (2022) 107187

Contents lists available at ScienceDirect

Electrochemistry Communications

journal homepage: www.elsevier.com/locate/elecom

Short Communication

Analytical impedance of two-layer oxygen transport media in a PEM fuel cell

Andrei Kulikovsky [a,1]

[a] Forschungszentrum Juelich GmbH, Theory and Computation of Energy Materials (IEK-13), D–52425 Jülich, Germany

ARTICLE INFO

Keywords:
PEM fuel cell
impedance
GDL
MPL
modeling

ABSTRACT

A model for impedance of oxygen transport in two porous layers A and B (GDL and MPL) positioned between the air channel and cathode catalyst layer in a PEM fuel cell is developed. Analytical solution shows that the system transport impedance cannot be split up into a sum of separate layer A and B impedances. The two-layer system works as a unified oxygen transport media. This result suggests that in general, impedance of all oxygen transport medias in a fuel cell are interdependent.

1. Introduction

Being non–invasive technique, electrochemical impedance spectroscopy (EIS) is widely used in PEM fuel cell research [1]. Over decades, deciphering of impedance spectra has been done using equivalent circuit method (see e.g. [2–4]). A standard software for fitting experimental impedance spectra using equivalent circuit is supplied with modern EIS–meters. However, the drawbacks of EC method are well known: any selected EC is not unique, there is no guarantee that good quality of fitting means relevance of the EC etc. Strong arguments against EC method have been given by Macdonald [5]. Nonetheless, due to its simplicity, EC technique is still used in research [6,7].

After pioneering numerical work of Springer et al. [8] and analytical paper of Eikerling and Kornyshev [9], development of physics–based impedance models has attracted much attention (see reviews [10,11]). Of particular interest are analytical impedance models, as they extend our understanding of fuel cell spectra and provide simple equations for spectra fitting.

In 1899, Warburg [12] derived a famous solution for impedance of semi–infinite transport layer attached to the electrode. Later, his approach has been used to derive impedance of a finite-length transport layer [1]. Analytical equations for impedance of gas diffusion layer (GDL) positioned between the cathode channel and catalyst layer have been derived in several works under various assumptions [13–15]. So far, however, micro-porous layer (MPL) has not been considered as a separate transport layer in PEMFC impedance modeling. Oxygen diffusion coefficient of MPL could be twice less, than the GDL diffusivity [16] and MPL impedance deserves special attention.

Below, analytical model for impedance of a PEMFC cathode equipped with two oxygen transport layers is developed. Analytical formula for impedance of the two-layer transport system is derived. Unexpectedly, this solution shows that the transport impedance of this system can not be split up into a sum of two impedances corresponding to layers A (GDL) and B (MPL). Rather, the two-layer system works as a unified transport media.

2. Model

2.1. Basic equations

The system schematic is shown in Fig. 1: two oxygen transport layers are placed between the air channel and the cathode catalyst layer (CCL). The layers are marked along the direction of oxygen flow: layer A (GDL) is attached to the channel, and layer B (MPL) is placed between layer A and CCL. Oxygen transport in layers A and B is described by the diffusion equations

$$\frac{\partial c_A}{\partial t} - D_A\frac{\partial^2 c_A}{\partial x^2} = 0, \quad D_A\frac{\partial c_A}{\partial x}\bigg|_{x=l_t+l_B} = D_B\frac{\partial c_B}{\partial x}\bigg|_{x=l_t+l_B} \qquad (1)$$

$$c_A(l_t + l_B + l_A) = c_h$$

$$\frac{\partial c_B}{\partial t} - D_B\frac{\partial^2 c_B}{\partial x^2} = 0, \quad D_B\frac{\partial c_B}{\partial x}\bigg|_{x=l_t} = \frac{j_0}{4F}, \quad c_B(l_t + l_B) = c_A(l_t + l_B) \qquad (2)$$

E-mail address: A.Kulikovsky@fz-juelich.de.
[1] ISE member

https://doi.org/10.1016/j.elecom.2021.107187
Received 3 November 2021; Received in revised form 4 December 2021; Accepted 16 December 2021
Available online 23 December 2021

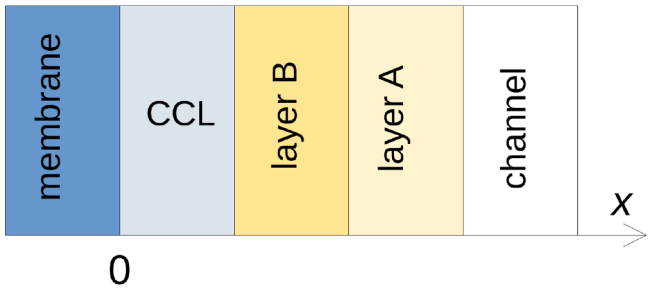

Fig. 1. Schematic of a PEMFC cathode with the GDL (layer A) and MPL (layer B).

Here, c_A, c_B are the oxygen concentrations in layers A and B, respectively, c_h is the oxygen concentration in channel, l_t is the CCL thickness, D_A and D_B are the oxygen diffusivities of layers A and B, l_A, l_B are the layers thicknesses, and j_0 is the cell current density.

The boundary conditions for Eq.(1) prescribe continuity of the oxygen flux at the layers A and B interface and fixed oxygen concentration in the channel. The boundary conditions for Eq.(2) mean stoichiometric oxygen flux at the CCL/layer B interface, and continuity of the oxygen concentration at the layer A/ layer B interface. The left boundary condition to Eq.(2) means that the oxygen transport through the CCL is assumed to be fast.

To relate oxygen transport with electric variables, we need the proton charge conservation equation. Assuming fast oxygen and proton transport in the CCL, this equation takes the form

$$C_{dl} l_t \frac{\partial \eta_0}{\partial t} - j_0 = -i_* l_t \left(\frac{c_1}{c_h^{in}}\right) \exp\left(\frac{\eta_0}{b}\right) \tag{3}$$

where C_{dl} is the double layer capacitance, η_0 is the positive by convention ORR overpotential, j_0 is the local cell current density, i_* is the ORR volumetric exchange current density, and c_1 is the oxygen concentration at the CCL/MPL interface, and c_h^{in} is the reference (inlet) oxygen concentration. Eq.(3) implies that η_0 is nearly constant through the CCL depth.

It is convenient to introduce dimensionless variables

$$\begin{gathered} \widetilde{t} = \frac{t}{t_*}, \quad \widetilde{x} = \frac{x}{l_t}, \quad \widetilde{c} = \frac{c}{c_h^{in}}, \quad \widetilde{j} = \frac{j}{i_* l_t}, \quad \widetilde{\eta} = \frac{\eta}{b}, \\ \widetilde{D}_{1,2} = \frac{4FD_{1,2}c_h^{in}}{i_* l_t^2}, \quad \widetilde{l}_{1,2} = \frac{l_{1,2}}{l_t}, \quad \widetilde{\omega} = \omega t_*, \quad \widetilde{Z} = \frac{Z i_* l_t}{b} \end{gathered} \tag{4}$$

where the time scale t_* is

$$t_* = \frac{C_{dl} b}{i_*}, \tag{5}$$

ω is the angular frequency of the applied AC signal, and Z is the impedance.

With the variables Eq.(4), Eqs.(1), (2) and (3) take the form

$$\begin{gathered} \mu^2 \frac{\partial \widetilde{c}_A}{\partial \widetilde{t}} - \widetilde{D}_A \frac{\partial^2 \widetilde{c}_A}{\partial \widetilde{x}^2} = 0, \quad \widetilde{D}_A \frac{\partial \widetilde{c}_A}{\partial \widetilde{x}}\Big|_{\widetilde{x}=1+\widetilde{l}_B} = \widetilde{D}_B \frac{\partial \widetilde{c}_B}{\partial \widetilde{x}}\Big|_{\widetilde{x}=1+\widetilde{l}_B}, \\ \widetilde{c}_A(1+\widetilde{l}_B+\widetilde{l}_A) = \widetilde{c}_h \end{gathered} \tag{6}$$

$$\mu^2 \frac{\partial \widetilde{c}_B}{\partial \widetilde{t}} - \widetilde{D}_B \frac{\partial^2 \widetilde{c}_B}{\partial \widetilde{x}^2} = 0, \quad \widetilde{D}_B \frac{\partial \widetilde{c}_B}{\partial \widetilde{x}}\Big|_{\widetilde{x}=1} = \widetilde{j}_0, \quad \widetilde{c}_B(1+\widetilde{l}_B) = \widetilde{c}_A(1+\widetilde{l}_B) \tag{7}$$

$$\frac{\partial \widetilde{\eta}_0}{\partial \widetilde{t}} - \widetilde{j}_0 = -\widetilde{c}_1 \exp\widetilde{\eta}_0 \tag{8}$$

where μ is the dimensionless parameter

$$\mu = \sqrt{\frac{4Fc_h^{in}}{C_{dl} b}} \tag{9}$$

Note that due to assumption of fast oxygen and proton transport in the CCL, all parameters in Eq.(8) are independent of $\widetilde{x}$.

2.2. Impedance

Substituting Fourier–transforms

$$\widetilde{\eta}_0 = \widetilde{\eta}^0 + \widetilde{\eta}^1(\widetilde{\omega})\exp(\mathrm{i}\widetilde{\omega}\widetilde{t}), \quad \widetilde{j}_0 = \widetilde{j}^0 + \widetilde{j}^1(\widetilde{\omega})\exp(\mathrm{i}\widetilde{\omega}\widetilde{t}), \quad \widetilde{c}_1 = \widetilde{c}_1^0 + \widetilde{c}_1^1(\widetilde{\omega})\exp(\mathrm{i}\widetilde{\omega}\widetilde{t}) \tag{10}$$

into Eq.(8), expanding exponent in Taylor series, neglecting term with the perturbations product, and subtracting the static equation, we get equation relating the small perturbation amplitudes $\widetilde{\eta}^1, \widetilde{j}^1$ and $\widetilde{c}_1^1$ in the $\widetilde{\omega}$–space:

$$\widetilde{j}^1 = \mathrm{i}\widetilde{\omega}\widetilde{\eta}^1 + \mathrm{e}^{\widetilde{\eta}_0}\left(\widetilde{c}_1^1 + \widetilde{c}_1^0\widetilde{\eta}^1\right). \tag{11}$$

Here, the superscripts 0 and 1 mark the static variables and the small perturbation amplitudes, respectively. Cathode side impedance is given by

$$\widetilde{Z} = \frac{\widetilde{\eta}^1}{\widetilde{j}^1} \tag{12}$$

Dividing Eq.(11) by $\widetilde{j}^1$, and using the static Tafel law $\widetilde{j}_0 = \widetilde{c}_1^0 \mathrm{e}^{\widetilde{\eta}_0}$ to eliminate $\mathrm{e}^{\widetilde{\eta}_0}$, we obtain equation for $\widetilde{Z}$:

$$1 = (\mathrm{i}\widetilde{\omega} + \widetilde{j}_0)\widetilde{Z} + \left(\frac{\widetilde{j}_0}{\widetilde{c}_1^0}\right)\frac{\widetilde{c}_1^1}{\widetilde{j}^1} \tag{13}$$

The remaining task is thus to calculate $\widetilde{c}_1^1$.

Eqs.(6), (7) are linear and hence we may directly write down the equations for small perturbation amplitudes $\widetilde{c}_A^1$ and $\widetilde{c}_B^1$:

$$\begin{gathered} \widetilde{D}_A \frac{\partial^2 \widetilde{c}_A^1}{\partial \widetilde{x}^2} = \mathrm{i}\widetilde{\omega}\mu^2 \widetilde{c}_A^1, \quad \widetilde{D}_A \frac{\partial \widetilde{c}_A^1}{\partial \widetilde{x}}\Big|_{\widetilde{x}=1+\widetilde{l}_B} = \widetilde{D}_B \frac{\partial \widetilde{c}_B^1}{\partial \widetilde{x}}\Big|_{\widetilde{x}=1+\widetilde{l}_B}, \\ \widetilde{c}_A^1(1+\widetilde{l}_B+\widetilde{l}_A) = 0 \end{gathered} \tag{14}$$

$$\widetilde{D}_B \frac{\partial^2 \widetilde{c}_B^1}{\partial \widetilde{x}^2} = \mathrm{i}\widetilde{\omega}\mu^2 \widetilde{c}_B^1, \quad \widetilde{D}_B \frac{\partial \widetilde{c}_B^1}{\partial \widetilde{x}}\Big|_{\widetilde{x}=1} = \widetilde{j}^1, \quad \widetilde{c}_B^1(1+\widetilde{l}_B) = \widetilde{c}_A^1(1+\widetilde{l}_B) \tag{15}$$

The right boundary condition for Eq.(14) means that the oxygen concentration perturbation in channel is zero. This condition holds if oxygen (air) flow stoichiometry is large.

3. Results and discussion

Solution of Eqs.(14), (15) is straightforward. For example,

$$\widetilde{c}_A(\widetilde{x}) = \frac{f_B \sqrt{\mathrm{i}} \sin\left(\mu\sqrt{\widetilde{\omega}/(2\widetilde{D}_A)}\,(\mathrm{i}-1)(1+\widetilde{l}_A+\widetilde{l}_B-\widetilde{x})\right)}{\mu\sqrt{\widetilde{D}_A\widetilde{\omega}}\cos\left(\mu\widetilde{l}_A\sqrt{-\mathrm{i}\widetilde{\omega}/\widetilde{D}_A}\right)} \tag{16}$$

where $f_B \equiv \widetilde{D}_B \partial \widetilde{c}_B^1/\partial \widetilde{x}|_{\widetilde{x}=1+\widetilde{l}_B}$. However, linking of these solutions through the boundary conditions involves rather tedious algebra. The result leads to the formula for $\widetilde{c}_1^1 = \widetilde{c}_B^1(1)$; upon substitution of $\widetilde{c}_1^1$ into Eq.(13), we get the system impedance

$$\widetilde{Z} = \frac{1}{\widetilde{j}_0 + \mathrm{i}\widetilde{\omega}} + \widetilde{Z}_{tr} \tag{17}$$

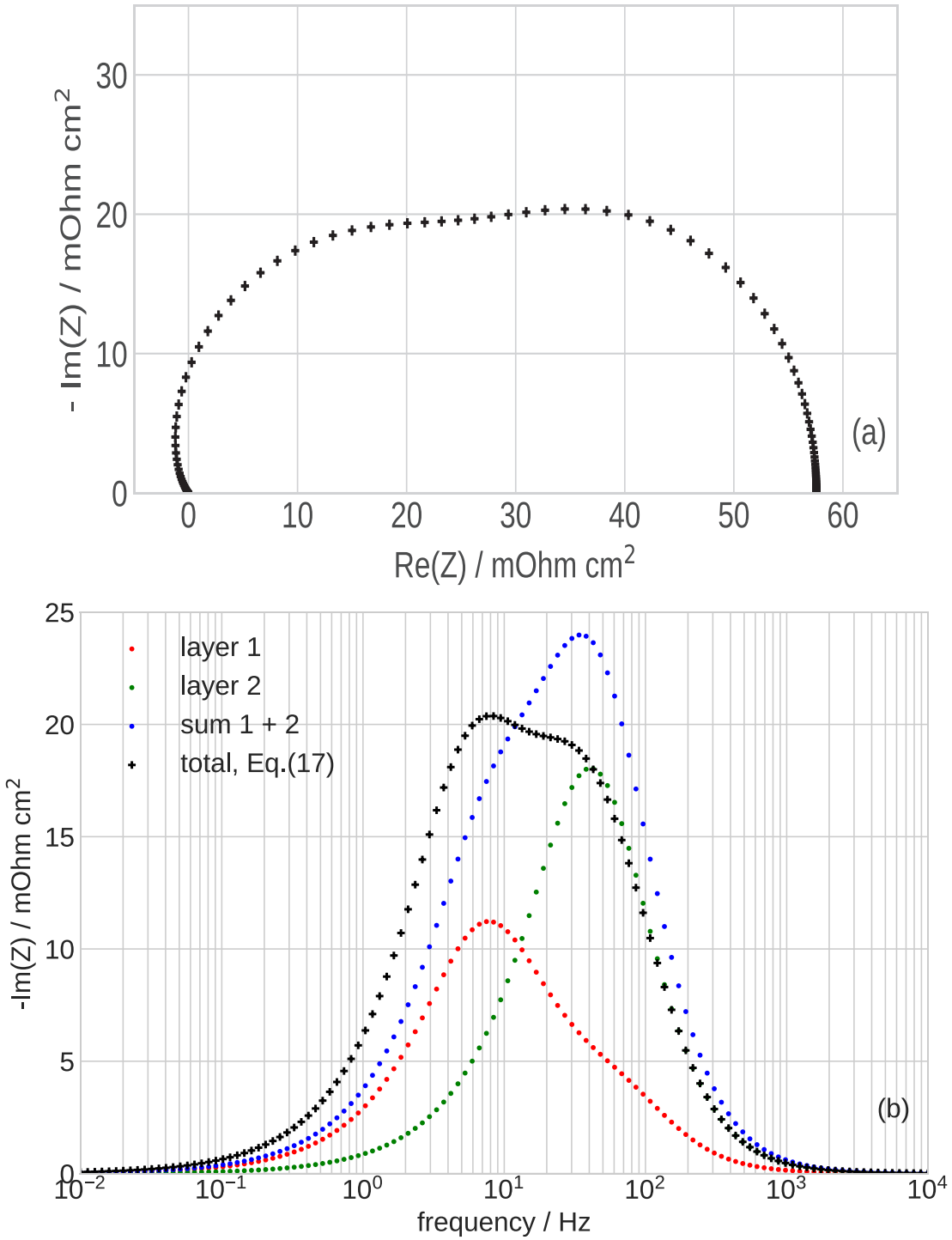

Fig. 2. (a) Nyquist spectrum of the total transport impedance, Eq.(18). (b) Frequency dependence of imaginary part of impedance of layer A (red dots), layer B (green dots), their sum (blue dots), and of the total impedance (black crosses). Parameters for calculations are listed in Table 1.

where the first term is faradaic impedance and the second term is transport impedance $\widetilde{Z}_{tr}$ of the GDL and MPL:

$$\widetilde{Z}_{tr}=\frac{\frac{\widetilde{l}_A\tanh\phi}{\widetilde{D}_A\phi}+\frac{\widetilde{l}_B\tanh\psi}{\widetilde{D}_B\psi}}{\widetilde{c}_1^0\left(1+\frac{\widetilde{\omega}}{j_0}\right)\left(1+\sqrt{\frac{\widetilde{D}_B}{\widetilde{D}_A}}\tanh(\phi)\tanh(\psi)\right)} \tag{18}$$

Here,

$$\phi=\mu\widetilde{l}_A\sqrt{\mathrm{i}\widetilde{\omega}/\widetilde{D}_A},\quad \psi=\mu\widetilde{l}_B\sqrt{\mathrm{i}\widetilde{\omega}/\widetilde{D}_B} \tag{19}$$

If the thicknesses and diffusion coefficients of the layers A and B are equal, we may set $\phi=\psi, \widetilde{D}_B=\widetilde{D}_A$ and Eq.(18) transforms to

$$\widetilde{Z}_{tr}^{A=B}=\frac{\tanh\left(2\mu\widetilde{l}_A\sqrt{\mathrm{i}\widetilde{\omega}/\widetilde{D}_A}\right)}{\widetilde{c}_1^0\mu\sqrt{\mathrm{i}\widetilde{\omega}\widetilde{D}_A}(1+\mathrm{i}\widetilde{\omega}/\widetilde{j}_0)} \tag{20}$$

which is impedance of a single transport layer of the double thickness

Table 1
The cell parameters used in calculations.

Layer A thickness l_A, cm	0.023
Layer B thickness l_B, cm	0.003
Layer A oxygen diffusivity D_A, cm^2 s^{-1}	$1{\cdot}10^{-2}$
Layer B oxygen diffusivity D_B, cm^2 s^{-1}	$1{\cdot}10^{-3}$
Catalyst layer thickness l_t, cm	$10{\cdot}10^{-4}$ (10 μm)
ORR Tafel slope b, V	0.03
Double layer capacitance C_{dl}, F cm^{-3}	20
Cell current density j_0, A cm^{-2}	0.5
Pressure	Standard
Cell temperature T, K	273 + 80

$2\widetilde{l}_A$ (Ref. [13]).

Further, at zero frequency, Eq.(17) reduces to the system resistivity

$$\widetilde{R} = \frac{1}{\widetilde{j}_0} + \frac{\widetilde{l}_A}{\widetilde{c}_1^0 \widetilde{D}_A} + \frac{\widetilde{l}_B}{\widetilde{c}_1^0 \widetilde{D}_B} \tag{21}$$

where the first term is faradaic resistivity, and the second and third terms are the static resistivities of layer A and B, respectively. We see that the static layer resistivities sum up. However, due to the product $\tanh(\phi)\tanh(\psi)$ in denominator of Eq.(18), the total transport impedance of the GDL and MPL *cannot* be represented as a sum of GDL and MPL contributions. The system GDL + MPL thus acts as a single integrated transport layer.

The Nyquist spectrum of the total transport impedance, Eq.(18), looks like two overlapping arcs (Fig. 2a). However, this spectrum is not a sum of the "pure" GDL and MPL contributions. Rather, the spectrum in Fig. 2a is a sum of two arcs, with the parameters of each arc being dependent on oxygen transport parameters of both the layers 1 and 2. Indeed, Eq.(18) can be expanded into a sum of two terms:

$$\widetilde{Z}_{tr} = \frac{\widetilde{l}_A \tanh(\phi)/(\widetilde{D}_A\phi)}{\widetilde{c}_1^0\left(1+\frac{\mathrm{i}\widetilde{\omega}}{\widetilde{j}_0}\right)\left(1+\sqrt{\frac{\widetilde{D}_B}{\widetilde{D}_A}}\tanh(\phi)\tanh(\psi)\right)} + \frac{\widetilde{l}_B \tanh(\psi)/(\widetilde{D}_B\psi)}{\widetilde{c}_1^0\left(1+\frac{\mathrm{i}\widetilde{\omega}}{\widetilde{j}_0}\right)\left(1+\sqrt{\frac{\widetilde{D}_B}{\widetilde{D}_A}}\tanh(\phi)\tanh(\psi)\right)} \tag{22}$$

However, each term of this sum contains the transport parameters of both layers 1 and 2, and variation of any of this parameters would change both the terms in Eq.(18).

To illustrate this behavior it is advisable to compare Eq.(18) with the sum of two single–layer impedances [13]

$$\widetilde{Z}_{A+B} = \frac{1}{\widetilde{c}_1^0(1+\mathrm{i}\widetilde{\omega}/\widetilde{j}_0)}\left(\frac{\widetilde{l}_A\tanh\phi}{\widetilde{D}_A\phi} + \frac{\widetilde{l}_B\tanh\psi}{\widetilde{D}_B\psi}\right) \tag{23}$$

The frequency dependencies of imaginary part of the separate layer A and B impedance, of their sum, Eq.(23), and of the total impedance, Eq.(18), are depicted in Fig. 2b. Comparison of blue and black curves in this Figure clearly shows that the total impedance is not a sum of impedances A and B, Eq.(23). For example, at the frequencies above 40 Hz, the total impedance is close to the sole layer B impedance, while the contribution of layer A (red points) is strongly damped (Fig. 2b).

This result suggests that in general, impedance of all oxygen transport medias in a fuel cell are interdependent. Channel, GDL, CCL, and eventually Nafion film covering Pt/C agglomerates in the CCL form a unified oxygen transport media with impedance of each element being dependent of transport parameters of all the other elements.

4. Conclusions

A model for oxygen transport impedance in the gas diffusion and micro–porous layers of a PEM fuel cell is developed. Analytical solution for impedance of the system GDL + MPL is derived. The Nyquist spectrum of the system transport impedance looks like two overlapping arcs; however, this impedance cannot be split up into a sum of separate GDL and MPL impedances.

Declaration of Competing Interest

The authors declare that they have no known competing financial interests or personal relationships that could have appeared to influence the work reported in this paper.

References

[1] A. Lasia, Electrochemical Impedance Spectroscopy and its Applications, Springer, New York, 2014.
[2] S.C. Page, A.H. Anbuky, S.P. Krumdieck, J. Brouwer, IEEE TRans. Energy Conv. 22 (2007) 764–773, https://doi.org/10.1109/TEC.2007.895857.
[3] A.M. Dhirde, N.V. Dale, H. Salehfar, M.D. Mann, T.-H. Han, IEEE Trans. Energy Conv. 25 (2010) 778–786, https://doi.org/10.1109/TEC.2010.2049267.
[4] J. Kim, J. Lee, B.H. Cho, IEEE Trans. Ind. Electron. 60 (2013) 5086–5094, https://doi.org/10.1109/TIE.2012.2226414.
[5] D. Macdonald, Electrochim. Acta 51 (2006) 1376–1388, https://doi.org/10.1016/j.electacta.2005.02.107.
[6] D.C. Sabarirajan, J. Liu, Y. Qi, A. Perego, A.T. Haug, I.V. Zenyuk, J. Electrochem. Soc. 167 (2020), 084521, https://doi.org/10.1149/1945-7111/ab927d.
[7] Q. Wang, Z. Hu, L. Xu, Q. Gan, J.L. 1, X. Du, M. Ouyang, Int. J. Energy Res. 45 (2021) 15948–15961. doi:10.1002/er.6825.
[8] T.E. Springer, T.A. Zawodzinski, M.S. Wilson, S. Gottesfeld, Characterization of polymer electrolyte fuel cells using AC impedance spectroscopy, J. Electrochem. Soc. 143 (1996) 587–599, https://doi.org/10.1149/1.1836485.
[9] M. Eikerling, A.A. Kornyshev, J. Electroanal. Chem. 475 (1999) 107–123, https://doi.org/10.1016/S0022-0728(99)00335-6.
[10] Z. Tang, Q.-A. Huang, Y.-J. Wang, F. Zhang, W. Li, A. Li, L. Zhang, J. Zhang, J. Power Sources 468 (2020), 228361, https://doi.org/10.1016/j.jpowsour.2020.228361.
[11] J. Huang, Y. Gao, J. Luo, S. Wang, C. Li, S. Chen, J. Zhang, J. Electrochem. Soc. 167 (2020), 166503, https://doi.org/10.1149/1945-7111/abc655.
[12] E. Warburg, Ann. Physik und Chemie 67 (1899) 493–499, https://doi.org/10.1002/andp.18993030302.
[13] A. Kulikovsky, O. Shamardina, J. Electrochem. Soc. 162 (2015) F1068–F1077, https://doi.org/10.1149/2.0911509jes.
[14] S. Chevalier, C. Josset, B. Auvity, J. Power Sources 407 (2018) 123–131, https://doi.org/10.1016/j.jpowsour.2018.10.039.
[15] S. Cruz-Manzo, P. Greenwood, J. Electrochem. Soc. 168 (2021), 074502, https://doi.org/10.1149/1945-7111/ac1031.
[16] C. Chan, N. Zamel, X. Li, J. Shen, Electrochimica Acta 39 (2012) 13–21, https://doi.org/10.1016/j.electacta.2011.12.110.